DOI: 10.1021/ma901668w

Macromolecules
ARTICLE

Model Transient Networks from Strongly Hydrogen-Bonded Polymers

Kathleen E. Feldman,[†] Matthew J. Kade,[‡] E. W. Meijer,[§] Craig J. Hawker,*[,‡,†] and Edward J. Kramer*[,†,⊥]

[†]*Materials Department, University of California, Santa Barbara, California 93106,* [‡]*Department of Chemistry and Biochemistry, University of California, Santa Barbara, California 93106,* [§]*Laboratory of Macromolecular and Organic Chemistry, Eindhoven University of Technology, Eindhoven, The Netherlands, and* [⊥]*Department of Chemical Engineering, University of California, Santa Barbara, California 93106*

Received July 28, 2009; Revised Manuscript Received August 28, 2009

ABSTRACT: Random copolymers consisting of *n*-butyl acrylate backbones with quadruple hydrogen-bonding side chains based on 2-ureido-4[1*H*]-pyrimidinone (UPy) have been synthesized via controlled radical polymerization and postpolymerization functionalization. Through this synthetic strategy high UPy monomer content (15 mol %) can be reached while maintaining low polydispersity and excellent control over molecular weight, providing model reversible networks with well-defined molecular architecture. Despite low T_gs and a lack of entanglements or crystallinity, these materials behave as thermoplastic elastomers through the strong but reversible association of UPy groups. Bulk properties such as the plateau modulus, tensile modulus, and relaxation time scale are primarily determined by the average distance between UPy's along the chain. Starting from a difunctional initiator, triblock copolymers can also be synthesized containing a homopolymer midblock and random copolymer end blocks, effectively concentrating the hydrogen-bonding groups near the chain ends. By controlling both the average composition and distribution of UPy's along the polymer chain, macroscopic material properties such as stiffness and resistance to creep can be independently tuned.

Introduction

Thermoplastic elastomers (TPEs) encompass a broad class of materials that can be processed, for example, by molding or extrusion, at elevated temperatures yet are elastomeric at ambient temperature. Typically such behavior arises through a phase-separated microstructure in which "hard" domains are bridged by "soft" rubbery chains; when a stress is applied to the material, the hard domains serve to pin the polymer chains and prevent macroscopic deformation, while the rubbery chains provide elasticity through the connectivity of the network. Transient networks, in which the junctions can be reversibly broken and re-formed, are interesting from both fundamental and applied standpoints; many reversibly associating polymers have been synthesized for use as rheological property modifiers or physical gels, and numerous theories have been presented[1−6] to describe their equilibrium and dynamic properties.

The reversible junctions in transient networks typically contain areas of hydrophobic associations,[7−10] hydrogen bonding,[11−17] metal−ligand interactions,[18,19] or ionic associations.[20,21] In many cases such junctions are poorly defined aggregates with unknown association strength and kinetics, but in a few transient network materials bulk properties have been directly correlated to defined polymer microstructure or well-characterized reversible interactions leading to important insights into the properties of these systems. In an early series of papers, Stadler and Freitas[11,22−24] studied the rheological behavior of polybutadienes lightly modified with double-hydrogen-bonding phenylurazole groups, finding that even with light substitution along the backbone the storage modulus plateau was broadened and shifted to lower frequencies (although the overall network properties were primarily dictated by the highly entangled polymer backbone and the crystallization of the phenyl urazole side chains). More recently, reversible networks based on metal−ligand coordination have been synthesized and the macroscopic material properties directly related to the coordination dynamics;[25−28] in this case it was found that formation of a strong network required not just a high association constant but also slow dynamics of the reversible bond. Additionally, supramolecular gels based on hydrogen bonding in ionic liquids have been demonstrated and their rheological properties related to the strength and number of hydrogen bonds as well as stoichiometry of donor and acceptor units.[29,30]

To broaden the scope and applicability of supramolecular polymer chemistry, many new strongly hydrogen-bonding moieties have been synthesized[31−37] and incorporated into network-forming materials.[12−15,38−41] The strength and specificity of multiple-hydrogen-bonded (MHB) groups vary widely, from weakly complementary pyridine−phenol pairs[42] to extremely strong, self-complementary 6-H-bonded dimers.[31] The 2-ureido-4[1*H*]-pyrimidinone (UPy) group first reported by Sijbesma et al.[12] was developed as a synthetically accessible, exceptionally strong ($K_{dim} = 6 \times 10^7$ M^{-1} in $CDCl_3$) quadruple-hydrogen-bonded dimer in order to create highly thermally responsive polymeric materials. By attaching UPy's to both ends of short, low-T_g oligomers, materials were produced which, at low temperature, bonded end to end to give high molecular weight polymer chains. On heating, the bonds between the oligomers dissociate and the material flows like a liquid. A number of other telechelic, UPy-based materials have been demonstrated to show similar behavior;[43−46] although useful, they generally rely on crystallization of the UPy dimers into long stacks to achieve mechanical stability, similar to the crystallization typically seen in segmented polyurethane thermoplastic elastomers. Later work showed that the nature of the linker joining the UPy group to the polymer chain dramatically affects the macroscopic properties. When an additional urea or urethane is present near the UPy group, lateral hydrogen bonding between dimers is enhanced,

*To whom correspondence should be addressed. E-mail: hawker@mrl.ucsb.edu (C.J.H.); edkramer@mrl.ucsb.edu (E.J.K.).

 Published on Web 09/17/2009

which results in the crystallization of the dimers into long stacks.[39] Alternately, bulky substituents near UPy's prevent such crystallization while linear alkyl chains enhance it.[40] In both cases, the presence of crystalline stacks (rather than simple pairwise UPy−UPy association) was shown to be crucial for network formation and good mechanical properties.

Examples of UPy-based segmented TPEs have also been presented in which the MHB groups comprise the "hard" segments of longer chains,[47,48] and several groups have also begun to incorporate UPy groups into higher molecular weight polymers as side chains via random copolymerization of a UPy-functional alkene[15] or methacrylate monomer.[14,38,49,50] Although the low solubility of the UPy methacrylate monomer limited its incorporation to 10 mol % or less, a higher degree of control over the bulk properties can be achieved via this route by varying any number of parameters including the concentration of UPy's in the chain, the total molecular weight, and the type of comonomer. In particular, it has been demonstrated that the melt viscosity and adhesive properties of random copolymers of *n*-butyl acrylate and UPy-methacrylate[14] together with the creep compliance of random copolymers of ethylhexyl methacrylate and UPy-methacrylate[49] can be widely varied by the concentration of UPy's along the backbone.

Although prior work has addressed the question of how the overall concentration of UPy monomer in random copolymers affects the bulk properties, most of the materials studied were synthesized via conventional radical polymerization leading to poor control over the chain architecture, molecular weight, and polydispersity. In this work we demonstrate a new synthetic strategy involving postpolymerization functionalization which allows well-defined precursor polymers to be prepared via atom transfer radical polymerization (ATRP) of *n*-butyl acrylate and a Boc-protected amine functional monomer. This allows for architectural control and higher incorporation of UPy's in the final polymers as well as effective control over the chain length and repeat unit distribution. By keeping the primary chain length below the entanglement molecular weight, the effects of the reversible interaction on the dynamics can be isolated from those due to reptation, in contrast with most prior examples of bulk transient networks. As a result, new questions about these materials, such as the relative importance of backbone molecular weight and overall concentration of UPy's, can be addressed. Additionally, we show that by controlling the distribution of UPy's along the chain through a triblock-like architecture it is possible to greatly improve the utility of such materials while minimizing the amount of functional monomer required.

Experimental Section

Methods. All synthetic procedures were performed under an inert atmosphere of dry nitrogen unless stated otherwise. *N,N*-Dimethylformamide (DMF) was dried over 4 Å molecular sieves. *tert*-Butyl 6-hydroxyhexylcarbamate was prepared as reported by Forbes et al.[51] Tris[2-(dimethylamino)ethyl]amine (Me_6TREN) was prepared as reported by Queffelec et al.[52] 2-(1-Imidazolylcarbonylamino)-6-methyl-4-[1*H*]-pyrimidinone was prepared as reported by Keizer et al.[53] Ethane-1,2-diyl bis(2-bromo-2-methylpropanoate) was synthesized as reported by Matyjaszewski et al.[54] *n*-Butyl acrylate was purified by passing over neutral alumina. Acryloyl chloride was distilled prior to use. All other chemicals were obtained from Aldrich and used as received.

Analytical TLC was performed on commercial Merck plates coated with silica gel GF254 (0.24 mm thick). ^{1}H NMR (500 MHz) and ^{13}C NMR (125 MHz) were performed on a Bruker AVANCE500 spectrometer at room temperature. Proton chemical shifts are reported in ppm downfield from tetramethylsilane (TMS). The following splitting patterns are designated as s, singlet; d, doublet; t, triplet; q, quartet; b, broad; m, multiplet; and dd, double doublet. Carbon chemical shifts are reported downfield from TMS using the resonance of the deuterated solvent as the internal standard.

Size exclusion chromatography was carried out at room temperature on a Waters chromatograph connected to a Waters 410 differential refractometer and six Waters Styragel columns (five HR-5 μm and one HWM-20 μm) using THF as eluent (flow rate: 1 mL/min). A Waters 410 differential refractometer and a 996 photodiode array detector were employed. The molecular weights of the polymers were calculated relative to linear polystyrene standards. Fourier transformed infrared spectroscopy was performed using a PerkinElmer Spectrum One spectrometer equipped with a Universal ATR accessory. Spectra are the sum of 16 scans acquired at a resolution of 4 cm^{-1}. Electrospray ionization time-of-flight (ESI-TOF) data were obtained on a Micromass QTOF2 quadrupole/time-of-flight tandem mass spectrometer.

Differential scanning calorimetry data were acquired on a TA Instruments Q2000 modulated DSC at a heating rate of 5 °C. Data presented are from the second heating after a single cycle from −75 to 100 °C. Rheological measurements were performed on an ARES rheometer from TA Instruments. Most samples were measured using a 25 mm cone and plate geometry (cone angle 0.1 rad), but for high-modulus materials it was necessary to use 8 mm parallel plates with a gap of 0.7 mm. Strain sweeps were performed at each temperature to ensure that measurements were made in the linear viscoelastic regime.

Synthesis. *6-(tert-Butoxycarbonylamino)hexyl Acrylate* (*t-Boc-AHA*). *tert*-Butyl 6-hydroxyhexylcarbamate (20 g, 92 mmol) and triethylamine (20 mL, 138 mmol) in dry methylene chloride (100 mL) were stirred at 0 °C. Acryloyl chloride (8.2 mL, 101 mmol) was added dropwise via syringe. The mixture was allowed to warm to room temperature and stirred overnight. Water was added (100 mL) to dissolve salts and hydrolyze any remaining acryloyl chloride, and the mixture stirred for 30 min. The organic layer was separated and washed with 1 N HCl (1 × 50 mL), $NaHCO_3$ (saturated, 1 × 50 mL), and brine (1 × 50 mL) and dried over sodium sulfate. The crude mixture was separated by flash column chromatography eluting with 1% methanol in methylene chloride to give a clear viscous oil (22.2 g, 89%). ^{1}H NMR ($CDCl_3$): d = 6.30 (dd, 1H), 6.04 (dd, 1H), 5.75 (dd, 1H), 4.65 (br, 1H), 4.07 (t, 2H), 3.03 (br, 2H), 1.60 (m, 2H), 1.42 (m, 2H), 1.36 (s, 9H), 1.34−1.25 ppm (m, 4H). ^{13}C NMR ($CDCl_3$): 166.2, 156.0, 130.4, 128.5, 78.8, 64.4, 40.4, 29.9, 28.4, 26.4, 25.6 ppm. FTR-IR (ATR): ν = 3364.9, 2932.9, 2860.9, 1710.0, 1692.7, 1636.5, 1619.4, 1516.3 cm^{-1}. ESI-MS (m/z): calcd: 294.17 ($M + Na^+$); found: 294.17 ($M + Na^+$), 310.14 ($M + K^+$).

Poly(n-butyl acrylate-r-Boc-aminohexyl acrylate). *n*-Butyl acrylate (3.24 g, 25.3 mmol), 6-(*tert*-butoxycarbonylamino)hexyl acrylate (0.726 g, 2.70 mmol), methyl 2-bromopropionate (31 mg, 1.9 mmol), and Me_6TREN (60 mg, 1.9 mmol) were sparged in a round-bottom flask with nitrogen for 10 min. CuBr (27 mg, 1.9 mmol) was added under flowing nitrogen. The flask was sealed and placed in a 70 °C oil bath for 45 min, then the polymerization was quenched by opening the flask to air and diluting with methylene chloride. The reaction mixture was washed with water (3 × 50 mL), 0.1 M EDTA (3 × 50 mL), and brine (1 × 50 mL), then dried over sodium sulfate, and evaporated. Residual monomer was removed by heating the polymer under high vacuum at 50 °C overnight to give P(nBA-*r*-*t*-Boc-AHA), M_n 24 600 g/mol, PDI 1.21 (THF GPC). ^{1}H NMR ($CDCl_3$): 4.68, 4.02, 3.10, 2.32, 1.90, 1.60, 1.43, 1.37, 0.93 ppm. ^{13}C NMR ($CDCl_3$): 174.5, 155.97, 79.0, 64.5, 41.4, 40.5, 36.3, 35.4, 30.6, 30.0, 28.4, 26.4, 25.6, 19.1, 13.7 ppm. FTR-IR (ATR): ν = 3391.3, 2932.9, 2933.8, 5869.4, 1723.6, 1636.6, 1516.4 cm^{-1}.

Poly(n-butyl acrylate-r-aminohexyl acrylate) (*TFA Salt*). P(nBA-*r*-*t*-Boc-AHA) (3.00 g) was dissolved in 25 mL of

Scheme 1. Synthesis of P(nBA-*r*-UPyA)

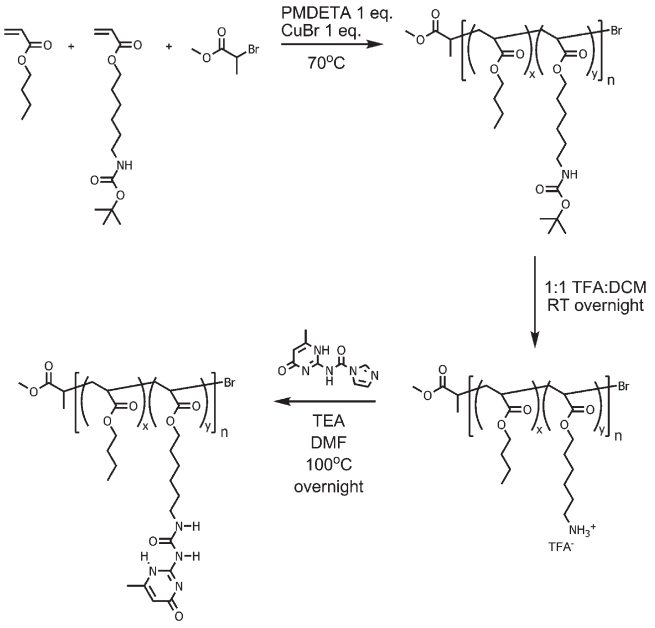

Scheme 2. Synthesis of Precursor Triblock Copolymer

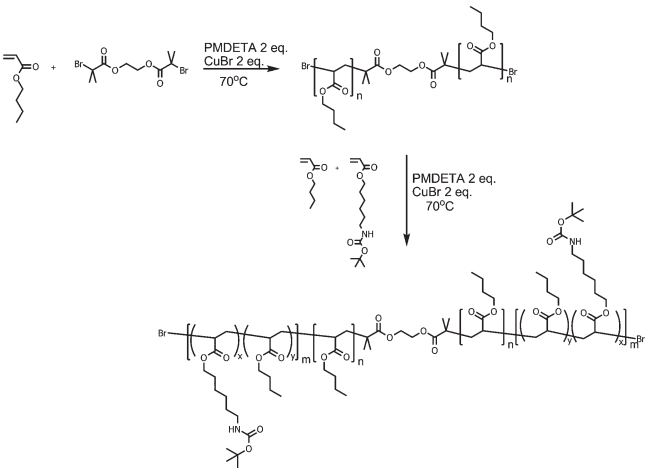

methylene chloride. TFA (25 mL) was added, and the mixture was stirred overnight. Solvent and excess TFA were removed by a rotavap, and residual TFA was removed by coevaporation with methanol followed by heating to 50 °C under high vacuum overnight to give P(nBA-*r*-AHA). ^{1}H NMR ($CDCl_3$): 7.77, 4.02, 3.04, 2.32, 1.90, 1.60, 1.37, 0.93 ppm. ^{13}C NMR ($CDCl_3$): 174.7, 64.7, 41.5, 40.0, 36.2, 35.2, 30.5, 28.1, 27.1, 25.7, 25.1, 19.0, 13.6 ppm. FTR-IR (ATR): ν = 2960.3, 2938.0, 2873.9, 1726.5, 1677.5, 1524.6 cm^{-1}.

Poly(n-butyl acrylate-r-UPy acrylate). P(nBA-*r*-AHA) (3.00 g) was dissolved in dry DMF (25 mL). Triethylamine (3 equiv per amine) and 2-(1-imidazolylcarbonylamino)-6-methyl-4-[1*H*]-pyrimidinone (1.5 equiv per amine) were added, and the mixture was heated to 100 °C overnight. Excess DMF was removed by a rotavap, and the polymer was precipitated into methanol to give P(nBA-*r*-UPyA). ^{1}H NMR ($CDCl_3$): 13.13, 11.87, 10.17, 5.82, 4.02, 3.25, 2.32, 1.90, 1.60, 1.37, 0.93 ppm. Limited solubility of UPy-functional polymers in $CDCl_3$ precluded the acquisition of reliable ^{13}C NMR spectra. FTR-IR (ATR): ν = 2957.6, 2932.4, 2872.7, 1729.3, 1698.4, 1661.8, 1586.2, 1524.6, 1448.2 cm^{-1}.

ABA Triblock Copolymers. Triblock copolymers were prepared by a similar method to the random copolymers as shown in Scheme 2. The midblock of PnBA was first polymerized using a difunctional initiator with 2 equiv of CuBr/Me_6TREN complex and purified by precipitation from acetone into cold methanol. The random copolymer end blocks were then poly merized from the PnBA macroinitiator via the procedure described previously, followed by deprotection of the Boc groups and functionalization with CDI-activated methylisocytosine.

Results and Discussion

Synthesis of Side-Chain UPy-Functionalized Polymers. Initial attempts at the synthesis of random copolymers from UPy-functional monomers met with limited success. A UPy-based acrylic monomer was synthesized, and random copolymers with *n*-butyl acrylate could be prepared at low UPy incorporation (< 5 mol %), although the PDIs were typically 1.3−1.5. With higher relative concentrations of UPy, however, the limited solubility of the monomer required the use of significant amounts of solvent in the polymerization. Even when fully soluble in the mixture, the polymerization did not proceed to any discernible degree, presumably due to a weak but significant interaction between the UPy monomer and copper catalyst under the ATRP conditions.

It was fundamentally important to increase the overall loading of UPy in the random copolymers, and to accomplish this, a postpolymerization functionalization strategy was developed as shown in Scheme 1. Rather than polymerizing the UPy-acrylate directly, Boc-protected 6-aminohexyl acrylate (*t*-Boc-AHA) was copolymerized with *n*-butyl acrylate. The two monomers are miscible liquids, and even at a feed ratio as high as 3:1 nBA:*t*-Boc-AHA the polymer composition closely matched the feed. Deprotection of the Boc groups with TFA proceeded smoothly; because of the possibility of transamidation between free amines and backbone esters, the TFA salts of the polymers were isolated rather than the neutralized analogues. Neutralization with triethylamine followed by immediate *in situ* reaction with CDI-activated methylisocytosine afforded the desired P(nBA-*r*-UPyA), which could be purified by precipitation into methanol. Triblock architectures were achieved through the use of a difunctional ATRP initiator which was used to first polymerize the midblock of nBA; random copolymer end blocks were then grown from Br-PnBA-Br difunctional macroinitiators.

Although deprotection of the Boc groups proceeded quantitatively as measured by ^{1}H NMR, functionalization yields were typically ∼75−85%, measured by comparing integrations of the alkylidene proton from the UPy side groups with the methylene adjacent to the backbone esters (see Supporting Information).

The characteristics of the synthesized polymers are given in Tables 1 and 2; the polymers are named according to the convention *a-m-c-f*, where *a* is either R for random copolymer or T for triblock, *m* is the number-average molecular weight in kg/mol, *c* is the overall mol % UPy monomer, and in the case of triblocks *f* is the volume fraction of the end blocks.

Effects of Chain Functionality. *n*-Butyl acrylate was chosen as the primary monomer in the random copolymers due to its low T_g, but it was expected that copolymerization with the UPy acrylate monomer might increase the overall T_g of the polymer, either due to the presence of hydrogen bonds and slowing of the chain dynamics or simply due to the steric effects on the backbone. As shown in Figure 1, a linear increase in T_g with increasing incorporation of UPy was observed, consistent with prior reports of UPy-functional random copolymers;[49,55] note, however, that even at high UPy loadings, the polymer T_g is still below room temperature and at least 40 °C below the lowest temperature for rheological measurements.

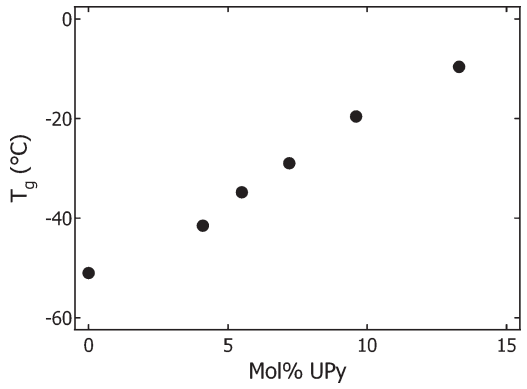

Figure 1. Relation between mole percent UPy monomer and polymer T_g; M_n for each polymer was ~24 kg/mol.

Table 1. P(nBA-*r*-UPyA) Random Copolymers

sample	M_n (precursor polymer)[a]	DP	mol % UPy[b]	M_n P(nBA-*r*-UPyA)[c]	*n* UPy's/chain	M_{UPy}
R-21-5.5	21 000	155	5.5	21 400	8.5	2520
R-25-7.2	24 600	178	7.2	25 300	13	1970
R-24-9.6	23 500	166	9.6	24 300	16	1530
R-21-13.3	21 100	144	13.3	22 100	19.1	1160
R-10-4.5	9 600	71	4.5	9 800	3.2	3040
R-18-4.1	18 400	137	4.1	18 700	5.6	3320
R-24-4.0	24 400	182	4.0	24 800	7.3	3390
R-33-4.3	32 500	242	4.3	33 000	10	3170

[a] THF GPC, PS equivalent. [b] ^{1}H NMR. [c] Calculated.

Table 2. P(nBA-*r*-UPyA)-*b*-PnBA-*b*-P(nBA-*r*-UPyA) Triblock Copolymers

sample	M_n (midblock PnBA)[a]	M_n total[a]	mol % UPy (end blocks)	mol % UPy (net)[b]	*n* UPy's/chain	f_{Ablock}
T-27-3.5-55	12 100	26 600	6.5	3.5	7.1	0.55
T-28-3.6-45	15 500	28 300	8.0	3.6	7.7	0.45
T-28-3.3-39	17 400	28 300	8.6	3.3	7.1	0.39

[a] THF GPC, PS equivalent. [b] ^{1}H NMR.

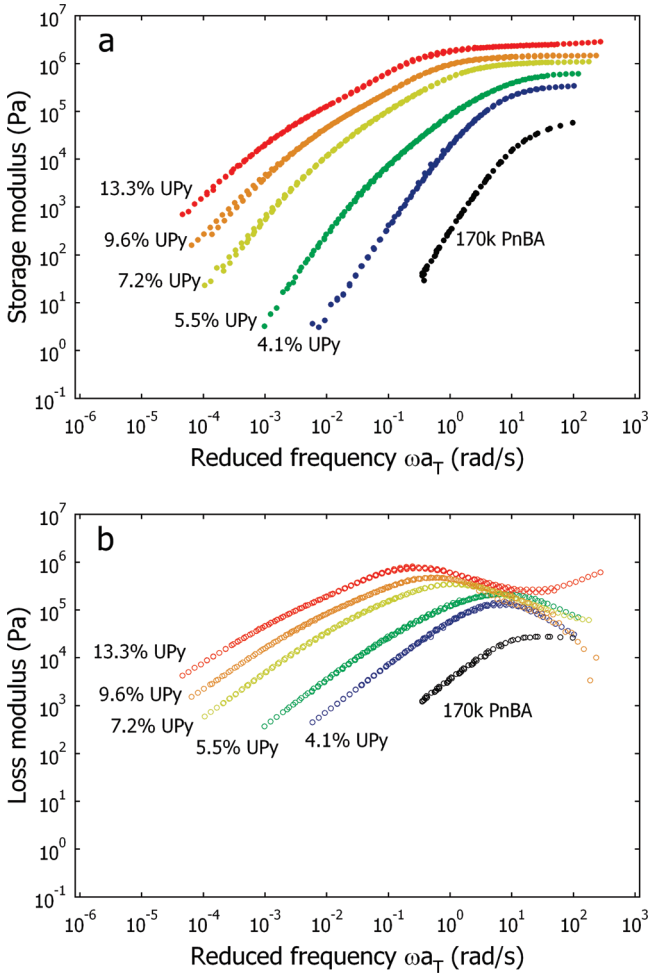

Figure 2. Storage (a) and loss (b) modulus master curves referenced to 50 °C showing the effect of increasing mole fraction of UPy acrylate at a molecular weight of ~24 kg/mol. A master curve for high molecular weight (170 kg/mol) PnBA homopolymer is included as a reference.

Figure 2 shows the overall effects on rheological properties of the increase in mole fraction of UPy acrylate in random copolymers at constant molecular weight (irreversible changes in the rheological data began to occur at temperatures greater than 120 °C so higher temperature data are not included in the master curves). It is immediately clear how significantly the polymer properties change with the addition of even a few mole percent of strongly hydrogen-bonding monomer. For reference, the master curve generated for a high molecular weight PnBA homopolymer (~170 kg/mol, well above M_e of 20 kg/mol[56]) is also shown; compared to all the UPy-functional polymers considered here it is the only one that is entangled, yet its dynamics are significantly faster and its plateau lower.

For the storage modulus master curves, each referenced to 50 °C (Figure 2a), time−temperature superposition (TTS) was satisfied in all cases, indicating that the governing relaxation processes all have similar temperature dependencies. At low fractions of UPy, the rheological behavior is uncomplicated and resembles an entangled homopolymer melt, with a small plateau at high reduced frequency and a terminal zone at low frequency with a slope near 2 (indicating liquidlike behavior). With increasing amounts of UPy, the plateau increases in magnitude and extends to much lower frequencies, and the rheological behavior becomes more complex; the terminal slope is no longer 2, meaning that, e.g., in the case of R-21-13.3 with 13.3 mol % UPy the longest relaxation time is greater than ~10^4 s at 50 °C. It should also be noted that in the construction of the master curves no vertical shift of the data was needed, demonstrating that the plateau modulus G_N is not a strong function of temperature and that because of the very large value of K_{dim}, there are very few free UPy's even at the highest temperatures measured.

Since the molecular weights of these polymers are all near the entanglement molecular weight of PnBA, the existence of a plateau modulus is entirely due to the presence of a transient network structure. Figure 3 shows the relationship between the plateau modulus G_N and mole fraction of UPy in polymers with comparable molecular weights ~24 kg/mol. A number of similar materials have been studied previously, including polymers containing UPy groups either at the chain ends or randomly spaced along the backbone. For these materials, thermoplastic elastomer-type behavior was attributed to the presence of stacked aggregates of UPy dimers (similar to the "hard" phase in polyurethane TPEs) which were observed through DSC and AFM. No melting transition has been observed by DSC in the P(nBA-*r*-UPyA) materials considered here, and wide-angle X-ray scattering experiments (WAXS, see Supporting Information) confirmed a lack of crystalline domains.

From the magnitude of the plateau modulus G_N it is possible to calculate a network strand density v_x and molecular weight between reversible network points M_c (M_n is the number-average molecular weight of the parent chains, and

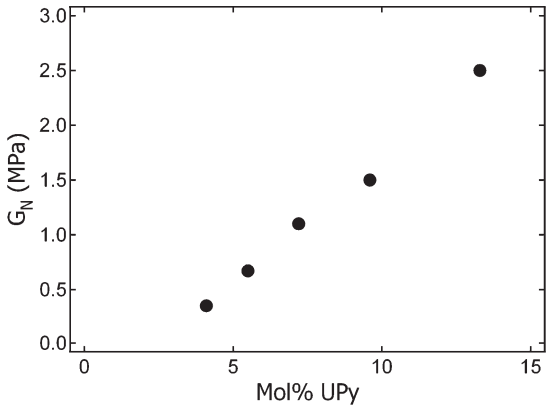

Figure 3. Plateau modulus G_N as a function of mole percent UPy acrylate at 50 °C.

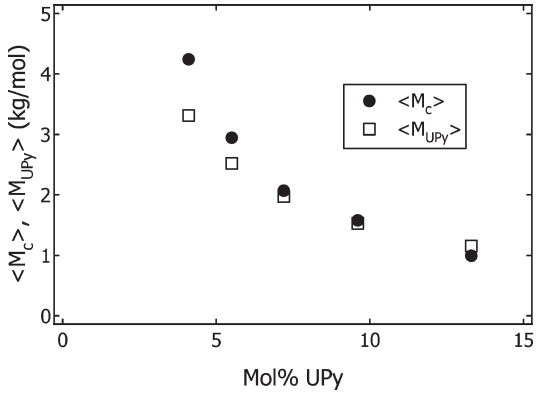

Figure 4. Comparison of M_c between network points and M_{UPy} between UPy's in polymers with increasing mole fraction UPy at constant molecular weight.

the term in parentheses is the standard (Flory) correction for the effect of loose chain ends which are not network active and thus do not contribute to the plateau modulus).

$$G_N = \nu_x RT = \frac{\rho RT}{M_c}\left(1 - \frac{2M_c}{M_n}\right) \quad (1)$$

In Figure 4, M_c is compared with the average molecular weight between UPy repeat units, M_{UPy}. Interestingly, as the mole fraction of UPy increases, the two values converge, indicating that a greater fraction of PnBA strands bounded by MHB groups are elastically active in the network. At ~7 mol % UPy and above it appears that every UPy side group is active, which indicates that at these high UPy concentrations loops between adjacent UPy's on the same chain are almost entirely absent.

Effects of Primary Molecular Weight. In contrast to the master curves changing significantly with increasing UPy content at constant molecular weight, when the UPy content is held constant and the molecular weight is increased, the master curve shapes look qualitatively similar as shown in Figure 5. In all cases the materials appear to be rheologically simple, displaying a plateau and narrow transition region to liquidlike terminal behavior, with the main differences being the breadth of the curve and the height and extent of the plateau (also note that in these samples T_g increases only slightly with molecular weight and increasing number of UPy's per chain, as shown in Figure 7).

Figure 6 shows how G_N relates to the molecular weight at a constant UPy content of ~4% UPy; at molecular weights higher than 9.6 kg/mol the plateau modulus remains fairly constant. This is understandable considering the average

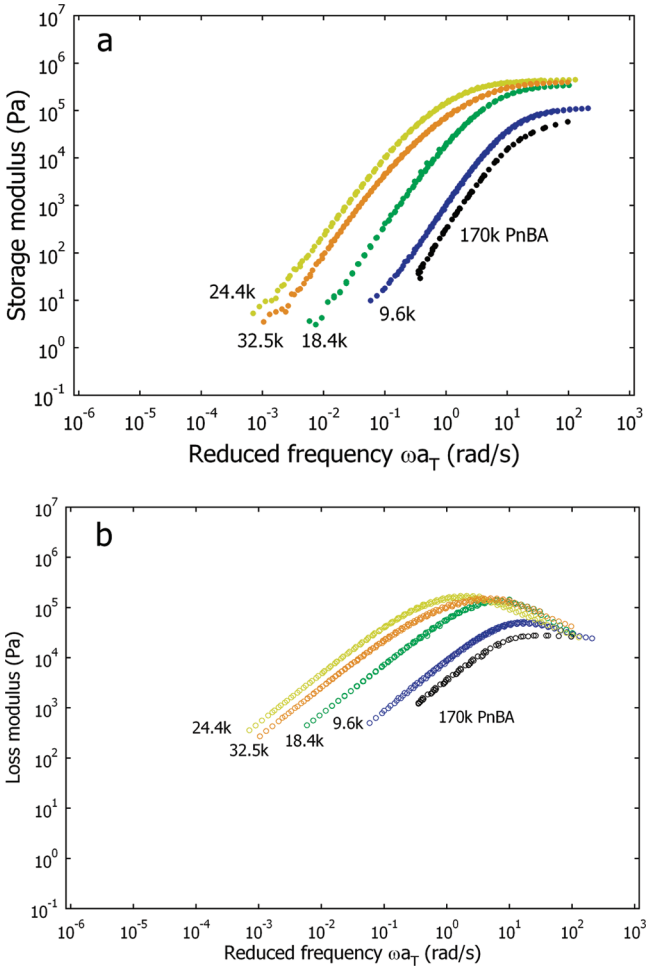

Figure 5. Storage (a) and loss (b) modulus master curves referenced to 50 °C showing the effect of increasing molecular weight at constant mole fraction UPy ~4%. A master curve for high molecular weight PnBA homopolymer is included as a reference.

number of UPy groups per chain in the 9.6 kg/mol sample (R-10-4.5) is between 3 and 4, and a connectivity of three is required for the formation of a network. With such a low average functionality there must be some chains which contain one or no UPy groups, neither of which contributes to the network structure. Despite the large difference in G_N between the lowest and higher molecular weight materials, Figure 7 shows that when corrected for chain ends the fraction of UPy's which are active in the network (reflected in the difference between M_c from eq 1 and M_{UPy}, Table 1) is relatively constant with molecular weight. Beyond a critical minimum, then, the primary chain molecular weight appears to minimally affect the bulk properties. Note, however, that all molecular weights in this series are expected to be unentangled. Much higher molecular weight polymers which would have entanglements as well as UPy groups are likely to show slower terminal relaxations.

Tuning Material Properties by the Distribution of MHB Groups. It is clear that the overall concentration of MHB groups, or more appropriately the average distance between them, influences the mechanical properties of associating random copolymers to a much greater extent than the length of the polymer chain. In prior studies of transient networks it has also been demonstrated that the distribution of associating groups along the polymer chain is an important parameter to control;[57−68] a "blocky" random structure leads to correlations between associating segments, slowing the

dynamics and producing stronger effective interchain interactions for a given average composition.

To achieve a similar "blocky" architecture in the current system, a PnBA homopolymer block was first polymerized from a difunctional initiator followed by growth of amino-containing random copolymer end blocks, as shown in Scheme 2, followed by UPy functionalization as described previously (Scheme 1). Because of the demonstrated control in these ATRP reactions, it is straightforward to match the total molecular weight and overall UPy content while varying the homopolymer midblock molecular weight. Accordingly, a series of triblock copolymers were synthesized with overall molecular weights of ~24 kg/mol and number of UPy's per chain of ~7 with increasing the midblock molecular weight and associated increase in the end block UPy concentration; the polymer characterization data are given in Table 2.

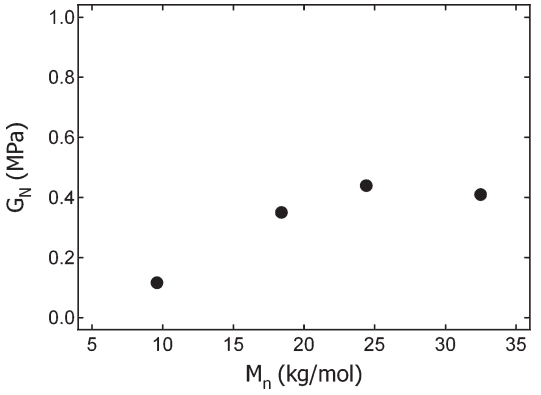

Figure 6. Plateau modulus G_N as a function of molecular weight at 4% UPy.

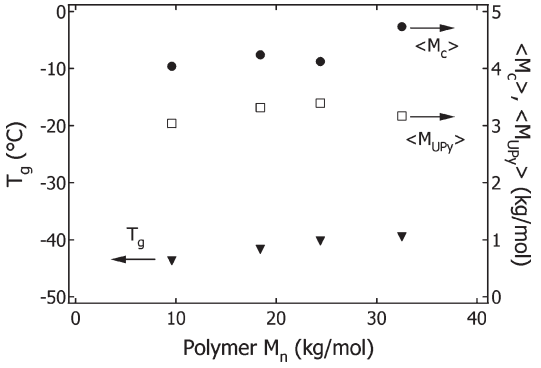

Figure 7. Comparison of M_c between network points and M_{UPy} between UPy's in polymers with increasing molecular weight at constant mole fraction UPy and relationship between primary chain molecular weight and T_g at UPy content of ~4 mol %.

It has been demonstrated previously[13,69] that, in addition to crystallization of hydrogen-bonding units in functional copolymers, microphase separation can play a major role in the bulk properties of such materials. Only a weak scattering peak is observed by small-angle X-ray scattering for each of the triblocks (Figure 8a), and the intensity of the peak increases with increasing concentration of the UPy's toward the chain ends. Because the scattering peak of T-28-3.3-39 (Figure 8b) shows only a minor change in intensity or position with temperature despite having the highest effective χN due to its greater chemical mismatch between the midblock and end blocks, it can be concluded that no microphase separation is taking place and the peak arises primarily from correlation hole scattering in the disordered melt.

From the rheological master curves shown in Figure 9 several observations can be made. By concentrating the UPy's near the ends of the chain, the plateau modulus G_N remains essentially constant but the width of the plateau is dramatically increased. This combination of effects leads to a significant decrease in the crossover frequency, and as a consequence these materials show solidlike behavior over much longer time scales than the corresponding random copolymer. Thus, despite the inhomogeneous UPy distribution, the network structure (i.e., the relative numbers of intra- and interchain hydrogen bonds) does not change appreciably, yet the dynamics are dramatically slowed. The key effect of controlling the distribution of UPy's along the chain is thus to decouple two macroscopic parameters, namely the stiffness (characterized by the plateau modulus) and relaxation time scales (reflected in the breadth of the master curve). By adopting a triblock-type architecture in which the UPy's are concentrated near the ends of the chain, the relaxations take place over longer and longer times, whereas the plateau modulus is determined by the average chain composition.

Dynamic Behavior and Reversible Network Theory. Dissociation of the hydrogen bonding for the polymer side chains is expected to be a thermally activated process showing Arrhenius-type behavior. The adherence to time−temperature superposition is thus possible because all of the materials considered here are well above their respective T_gs and the homopolymer relaxation processes follow an Arrhenius relation, but one with a much lower activation energy. This point is confirmed in Figure 10, which shows the temperature dependence of the shift factors a_T used to construct the rheological master curves. Plotting a_T versus inverse temperature yields a straight line in all cases,

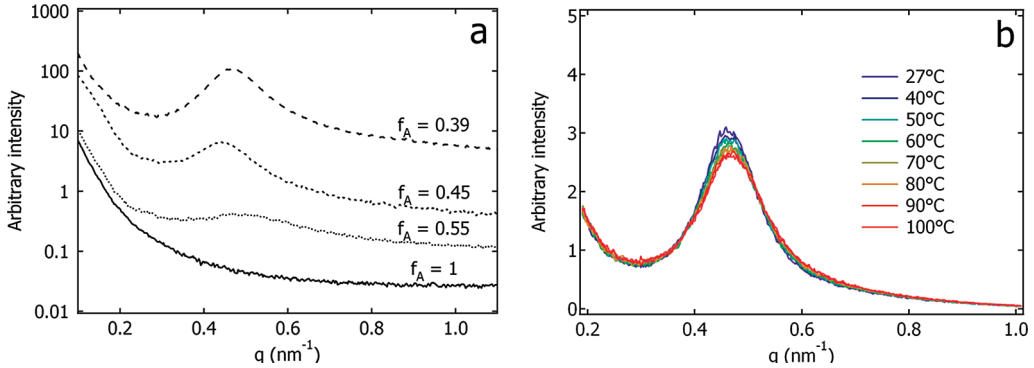

Figure 8. Small-angle X-ray scattering data: (a) room temperature scattering of triblocks, traces have been vertically shifted for clarity; (b) variable temperature (VT-SAXS) scattering of T-28-3.3-39).

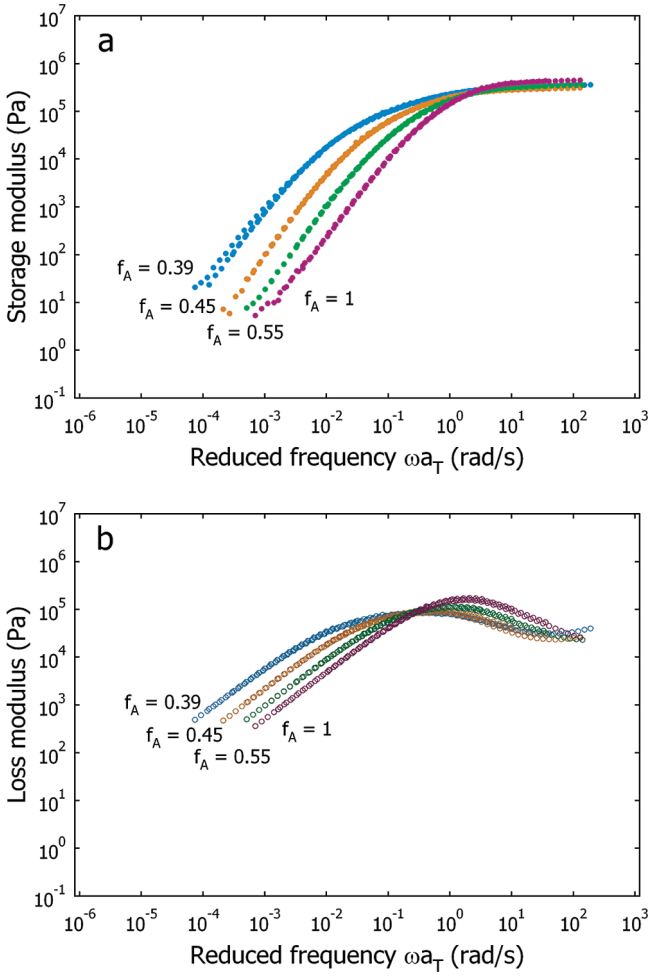

Figure 9. Storage (a) and loss (b) modulus master curves of triblock copolymers referenced to 50 °C. f_A refers to the weight fraction of the random copolymer end blocks.

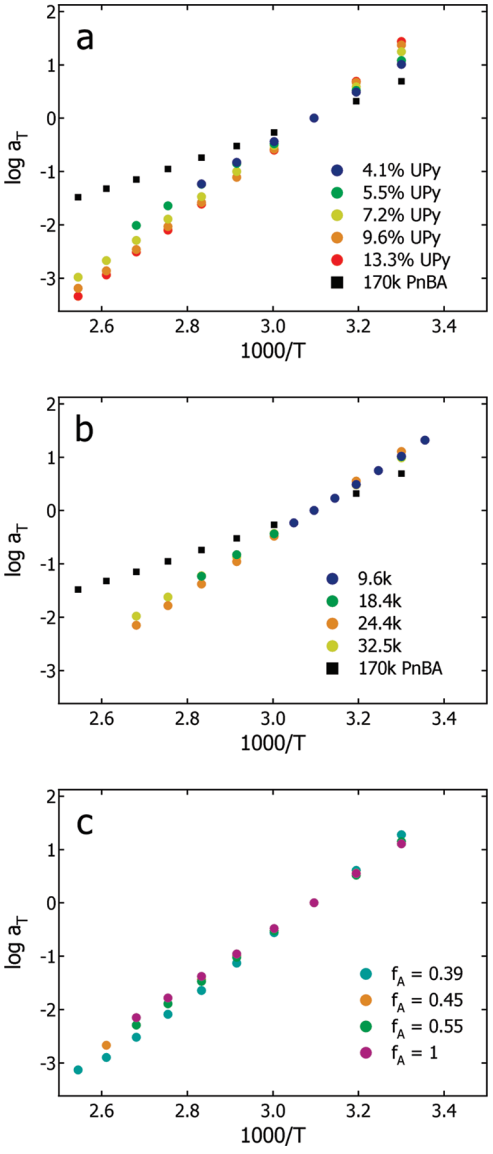

Figure 10. Temperature dependence of shift factors used in generating the master curves of Figure 2.

indicating Arrhenius behavior, and the slope of the line can be used to calculate a flow activation energy E_a (shown in Figure 11). It is immediately clear that the UPy-based materials show a much stronger temperature dependence than PnBA homopolymer and that E_a increases slightly with UPy content, each manifestations of the thermoreversibility of hydrogen bonding. Figure 11 also demonstrates that this small increase in flow activation energy with UPy content is correlated with the (local) average distance between UPy's along the chain—at a given average distance between UPy groups the E_a values for the triblock copolymers and the random copolymers are nearly the same.

Many theoretical treatments of reversibly associating polymer solutions have been proposed, but the most relevant to the current system was developed by Rubinstein and Semenov.[1,2,70] Although the majority of their work addresses associating polymers in dilute or semidilute solution, the theory has also been extended to very high concentrations, far from the gel point (in analogy to the polymer melt). In the limit of high binding strength, intramolecular associations (loops) were predicted to become significant, but at high polymer concentrations the majority of associations are intermolecular. More importantly, because of the very low concentration of unassociated stickers, a given pair will break and re-form many times before finally separating, leading to an effective bond lifetime τ_b^* greater than the bare bond lifetime τ_b. In this work τ_b^* is measured from the frequency at which the storage modulus has dropped to 90% of its plateau value (see the Supporting Information for a comparison with an alternative measure of τ_b, namely the network strand lifetime measured at the crossover frequency). The theory also predicts a longest relaxation time greater than τ_b^* arising from the fact that the associating polymers are essentially Rouse-like chains—the stickers can be considered "beads" with a higher monomer friction coefficient and an effective bead jump time of τ_b^*, and the "springs" are the spacers between them.

From Figure 12a it can be seen that the effective bond lifetime τ_b^* increases significantly with increasing concentration of UPy in the network. The lifetime of small molecule UPy dimers in solution[40] was previously found to depend strongly on the polarity of the solvent and ranged from 80 ms (chloroform saturated with water) to 1.7 s (toluene). The PnBA environment considered here is relatively polar, and so the bare lifetime should be low; R-10-4.5, which showed a dropoff of the plateau at the highest frequency, provides an upper limit to the UPy dimer lifetime τ_b in PnBA at 25 °C of 1.2 s, although NMR exchange experiments would be necessary to determine its

actual value.[71] In every other material studied here, the effective bond lifetime is significantly higher. From Figure 12b it is also clear that τ_b^* depends somewhat on the UPy distribution, suggesting that the average (local) distance between stickers along the chain influences the dynamic behavior in these materials. Presumably as the distance between two stickers along the chain is decreased, the relaxation of stress will require their concurrent unbinding. As a result, increasing the local concentration of UPy's leads to a correlation of their dynamics (also reflected in the flow activation energy, Figure 11), and as previously demonstrated,[27] it is the dynamics of unbinding and binding that dominate the macroscopic response.

Within the Rubinstein and Semenov theory, at frequencies lower than that corresponding to τ_b^* the polymer chains are considered Rouse-like. The Rouse model predictions for the frequency dependence of G' and G'' are as follows:[72]

$$G'(\omega) \approx \frac{k_B T \nu_x}{n_s} \frac{(\omega\tau_{max})^2}{\sqrt{[1+(\omega\tau_{max})^2][\sqrt{1+(\omega\tau_{max})^2}+1]}} \quad (2)$$

$$G''(\omega) \approx \frac{k_B T \nu_x}{n_s} (\omega\tau_{max})^2 \sqrt{\frac{\sqrt{1+(\omega\tau_{max})^2}+1}{1+(\omega\tau_{max})^2}} \quad (3)$$

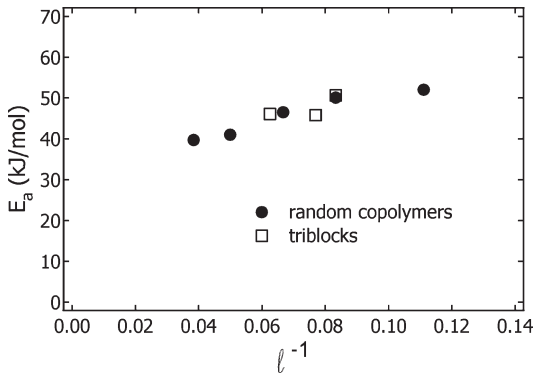

Figure 11. Activation energies E_a calculated from the temperature dependence of a_T (l: average degree of polymerization between UPy's; in the case of triblocks l is calculated based on the local UPy concentration within the random copolymer end blocks).

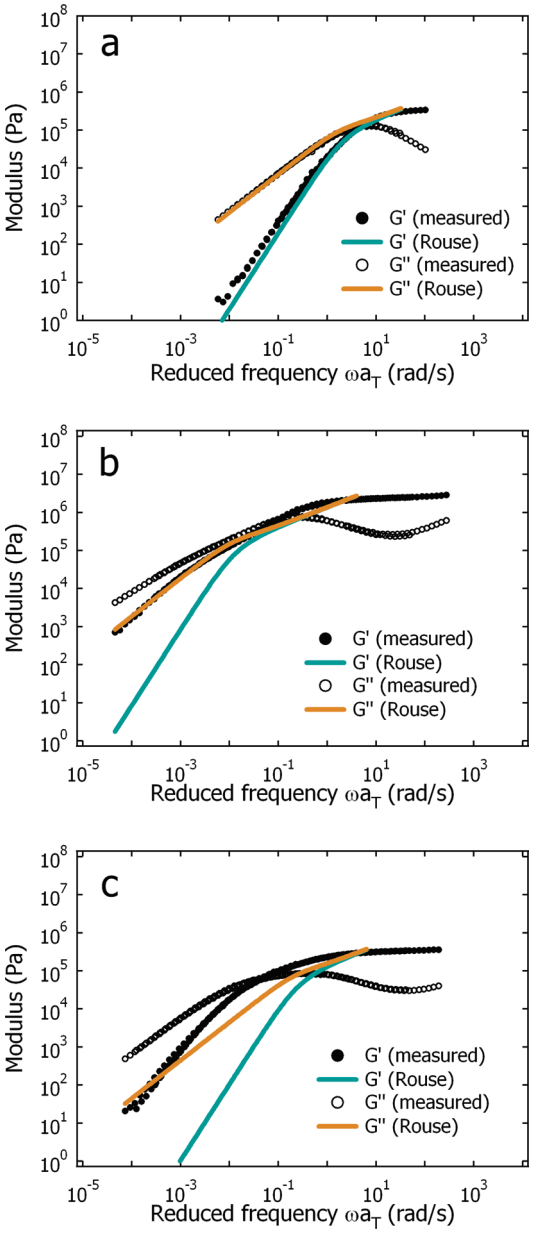

Figure 13. Storage and loss modulus master curves (symbols) and predicted Rouse-like behavior (lines) for three representative samples: (a) R-18-4.1; (b) R-21-13.3; (c) T-28-3.3-39.

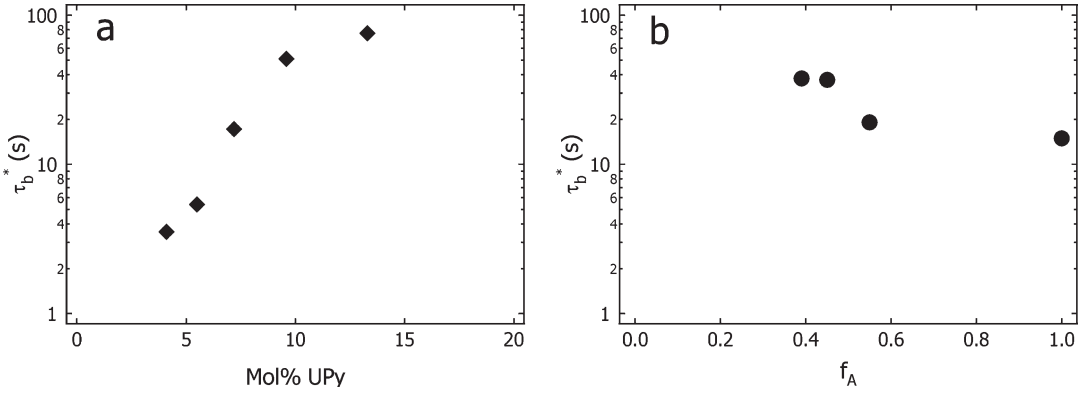

Figure 12. Effective bond lifetime at 25 °C calculated as described in the text: (a) random copolymers with increasing UPy content M_n ~24 kg/mol; (b) triblock copolymers with N_{UPy} ~7, M_n ~ 24 kg/mol, and decreasing PnBA midblock length.

where ν is the network strand density, $\tau_{max} = \tau_b^*(n_s)^2$, and n_s is the number of stickers per chain that are active in the network. Figure 13 compares the predicted Rouse-like behavior with the rheological master curves for several representative samples. Although the theory works well for random copolymers with very low UPy content, the predictions fail at high UPy incorporation, and when the architecture is blocky, where relaxations take place over much longer times than expected based simply on n_s and τ_b^*. It is clear, then, that existing theories must be modified or a new theory developed to describe both the general trends in dynamics in such materials and the dramatic effects of chain architecture.

Conclusions

A new strategy for the synthesis of random copolymers containing *n*-butyl acrylate and a strongly hydrogen-bonding side chain based on 2-ureido-4[1*H*]-pyrimidinone (UPy) has been presented. Parent polymers containing nBA and Boc-protected 6-aminohexyl acrylate were synthesized via ATRP, and postpolymerization functionalization allows much higher levels of incorporation of UPy groups to be achieved when compared to traditional strategies. All the materials currently considered are below the entanglement molecular weight of PnBA, yet all showed high frequency/low temperature rheological behavior indicative of a transient network structure whose plateau modulus depends primarily on the average concentration of UPy's along the chain. Under uniaxial extension, the initial modulus and strain at break also depended strongly on UPy concentration. Comparison of the crossover frequencies showed that with increasing UPy content the effective bond lifetime within the transient network increased, in keeping with prior theoretical predictions. At lower frequencies both the storage and loss moduli deviated from the behavior expected of simple entangled melts, indicating the presence of unusually long relaxation times. In contrast, it was shown that keeping the average UPy concentration along the chain constant, and increasing the molecular weight had only minor effects on the bulk properties. By altering the macromolecular architecture and distribution of UPy's along the chain, dramatic changes in the dynamic behavior were observed. A series of polymers were synthesized keeping the overall molecular weight and total number of UPy's per chain constant; however, the weight fraction of the PnBA homopolymer midblock was varied which concentrates the UPy's near the ends of the chains. The effective bond lifetime in these materials was strongly dependent on the chain architecture, leading to elastomeric behavior over much longer time scales. Understanding these trends will allow for the design of new UPy-based thermoplastic elastomers that fulfill the twin desires of optimal property enhancement while minimizing the amount of functional units (UPy) employed.

Acknowledgment. This work was supported by the MRSEC Program of the National Science Foundation under Award DMR05-20415. K.E.F. acknowledges support from NDSEG, NSF, and CSP Technologies fellowships.

Supporting Information Available: ^{1}H NMR, FTIR, and WAXS characterization of random copolymers and a comparison of the two methods for measuring τ_b. This material is available free of charge via the Internet at http://pubs.acs.org.

References and Notes

(1) Rubinstein, M.; Semenov, A. N. *Macromolecules* **1998**, *31*, 1386–1397.
(2) Semenov, A. N.; Rubinstein, M. *Macromolecules* **1998**, *31*, 1373–1385.
(3) Green, M.; Tobolsky, A. *J. Chem. Phys.* **1946**, *14*, 80–92.
(4) Lodge, A. *Trans. Faraday Soc.* **1956**, *52*, 120–130.
(5) Tanaka, F.; Edwards, S. *Macromolecules* **1992**, *25*, 1516–1523.
(6) Leibler, L.; Rubinstein, M.; Colby, R. *Macromolecules* **1991**, *24*, 4701–4707.
(7) Annable, T.; Buscall, R.; Ettelaie, R. *Colloids Surf., A* **1996**, *112*, 97–116.
(8) Annable, T.; Buscall, R.; Ettelaie, R.; Whittlestone, D. *J. Rheol.* **1993**, *37*, 695–726.
(9) Bagger-Jörgensen, H.; Coppola, L.; Thuresson, K.; Olsson, U.; Mortensen, K. *Langmuir* **1997**, *13*, 4204–4218.
(10) Tam, K.; Jenkins, R.; Winnik, M.; Bassett, D. *Macromolecules* **1998**, *31*, 4149–4159.
(11) Stadler, R.; Freitas, L. D. *Polym. Bull.* **1986**, *15*, 173–179.
(12) Sijbesma, R. P.; Beijer, F. H.; Brunsveld, L.; Folmer, B. J. B.; Hirschberg, J.; Lange, R. F. M.; Lowe, J. K. L.; Meijer, E. W. *Science* **1997**, *278*, 1601–1604.
(13) Sivakova, S.; Bohnsack, D. A.; Mackay, M. E.; Suwanmala, P.; Rowan, S. J. *J. Am. Chem. Soc.* **2005**, *127*, 18202–18211.
(14) Yamauchi, K.; Lizotte, J. R.; Long, T. E. *Macromolecules* **2003**, *36*, 1083–1088.
(15) Rieth, L. R.; Eaton, R. F.; Coates, G. W. *Angew. Chem., Int. Ed.* **2001**, *40*, 2153–2156.
(16) Cordier, P.; Tournilhac, F.; Soulie-Ziakovic, C.; Leibler, L. *Nature* **2008**, *451*, 977–980.
(17) Montarnal, D.; Tournilhac, F.; Hidalgo, M.; Couturier, J.-L.; Leibler, L. *J. Am. Chem. Soc.* **2009**, *131*, 7966–7967.
(18) Beck, J.; Rowan, S. *J. Am. Chem. Soc.* **2003**, *125*, 13922–13923.
(19) Weng, W.; Beck, J. B.; Jamieson, A. M.; Rowan, S. J. *J. Am. Chem. Soc.* **2006**, *128*, 11663–11672.
(20) MacKnight, W.; Earnest, T. *Macromol. Rev.* **1981**, *16*, 41–122.
(21) Eisenberg, A.; Hird, B.; Moore, R. B. *Macromolecules* **1990**, *23*, 4098–4107.
(22) Stadler, R.; Freitas, L. D. *Colloid Polym. Sci.* **1988**, *266*, 1102–1109.
(23) Stadler, R.; Freitas, L. D. *Macromolecules* **1989**, *22*, 714–719.
(24) Stadler, R.; Freitas, L. D. *Colloid Polym. Sci.* **1986**, *264*, 773–778.
(25) Loveless, D.; Jeon, S.; Craig, S. *Macromolecules* **2005**, *38*, 10171–10177.
(26) Serpe, M. J.; Craig, S. L. *Langmuir* **2007**, *23*, 1626–1634.
(27) Yount, W.; Loveless, D.; Craig, S. *Angew. Chem., Int. Ed.* **2005**, *44*, 2746–2748.
(28) Yount, W.; Loveless, D.; Craig, S. *J. Am. Chem. Soc.* **2005**, *127*, 14488–14496.
(29) Noro, A.; Matsushita, Y.; Lodge, T. P. *Macromolecules* **2008**, *41*, 5839–5844.
(30) Noro, A.; Matsushita, Y.; Lodge, T. P. *Macromolecules* **2009**, *42*, 5802–5810.
(31) Zeng, H.; Yang, X.; Brown, A.; Martinovic, S.; Smith, R.; Gong, B. *Chem. Commun.* **2003**, 1556–1557.
(32) Park, T.; Todd, E. M.; Nakashima, S.; Zimmerman, S. C. *J. Am. Chem. Soc.* **2005**, *127*, 18133–18142.
(33) Lafitte, V.; Aliev, A.; Horton, P.; Hursthouse, M.; Bala, K.; Golding, P.; Hailes, H. *J. Am. Chem. Soc.* **2006**, *128*, 6544–6545.
(34) Corbin, P.; Zimmerman, S. *J. Am. Chem. Soc.* **1998**, *120*, 9710–9711.
(35) Zhao, X.; Wang, X.; Jiang, X.; Chen, Y.; Li, Z.; Chen, G. *J. Am. Chem. Soc.* **2003**, *125*, 15128–15139.
(36) Li, X.; Jiang, X.; Wang, X.; Li, Z. *Tetrahedron* **2004**, *60*, 2063–2069.
(37) Ong, H.; Zimmerman, S. *Org. Lett.* **2006**, *8*, 1589–1592.
(38) Yamauchi, K.; Kanomata, A.; Inoue, T.; Long, T. E. *Macromolecules* **2004**, *37*, 3519–3522.
(39) Botterhuis, N. E.; van Beek, D. J. M.; van Gemert, G. M. L.; Bosman, A. W.; Sijbesma, R. P. *J. Polym. Sci., Part A: Polym. Chem.* **2008**, *46*, 3877–3885.
(40) Söntjens, S. H. M.; Sijbesma, R. P.; van Genderen, M. H. P.; Meijer, E. W. *J. Am. Chem. Soc.* **2000**, *122*, 7487–7493.
(41) Li, J.; Viveros, J.; Wrue, M.; Anthamatten, M. *Adv. Mater.* **2007**, *19*, 2851–2855.
(42) Tang, C.; Lennon, E. M.; Fredrickson, G. H.; Kramer, E. J.; Hawker, C. J. *Science* **2008**, *322*, 429–432.
(43) Lange, R. F. M.; Gurp, M. V.; Meijer, E. W. *J. Polym. Sci., Part A: Polym. Chem.* **1999**, *37*, 3657–3670.
(44) Hirschberg, J. H. K. K.; Beijer, F. H.; van Aert, H. A.; Magusin, P. C. M. M.; Sijbesma, R. P.; Meijer, E. W. *Macromolecules* **1999**, *32*, 2696–2705.

(45) Dankers, P. Y. W.; Zhang, Z.; Wisse, E.; Grijpma, D. W.; Sijbesma, R. P.; Feijen, J.; Meijer, E. W. *Macromolecules* **2006**, *39*, 8763–8771.
(46) van Beek, D.; Spiering, A.; Peters, G.; teNijenhuis, K.; Sijbesma, R. *Macromolecules* **2007**, *40*, 8464–8475.
(47) Söntjens, S. H. M.; Renken, R. A. E.; van Gemert, G. M. L.; Engels, T. A. P.; Bosman, A. W.; Janssen, H. M.; Govaert, L. E.; Baaijens, F. P. T. *Macromolecules* **2008**, *41*, 5703–5708.
(48) van Beek, D. J. M.; Gillissen, M. A. J.; van As, B. A. C.; Palmans, A. R. A.; Sijbesma, R. P. *Macromolecules* **2007**, *40*, 6340–6348.
(49) Elkins, C. L.; Park, T.; McKee, M. G.; Long, T. E. *J. Polym. Sci., Part A: Polym. Chem.* **2005**, *43*, 4618–4631.
(50) McKee, M. G.; Elkins, C. L.; Park, T.; Long, T. E. *Macromolecules* **2005**, *38*, 6015–6023.
(51) Forbes, C. C.; DiVittorio, K. M.; Smith, B. D. *J. Am. Chem. Soc.* **2006**, *128*, 9211–9218.
(52) Queffelec, J.; Gaynor, S.; Matyjaszewski, K. *Macromolecules* **2000**, *33*, 8629–8639.
(53) Keizer, H. M.; Sijbesma, R. P.; Meijer, E. M. *Eur. J. Org. Chem.* **2004**, 2553–2555.
(54) Matyjaszewski, K.; Miller, P.; Pyun, J.; Kickelbick, G.; Diamanti, S. *Macromolecules* **1999**, *32*, 6526–6535.
(55) Yamauchi, K.; Lizotte, J. R.; Long, T. E. *Macromolecules* **2002**, *35*, 8745–8750.
(56) Tobing, S. D.; Klein, A. *J. Appl. Polym. Sci.* **2001**, *79*, 2230–2244.
(57) Yoshida, T.; Kanaoka, S.; Watanabe, H.; Aoshima, S. *J. Polym. Sci., Part A: Polym. Chem.* **2005**, *43*, 2712–2722.
(58) Biggs, S.; Selb, J.; Candau, F. *Langmuir* **1992**, *8*, 838–847.
(59) Candau, F.; Selb, J. *Adv. Colloid Interface Sci.* **1999**, *79*, 149–172.
(60) Caputo, M.; Selb, J.; Candau, F. *Polymer* **2004**, *45*, 231–240.
(61) Hill, A.; Candau, F.; Selb, J. *Macromolecules* **1993**, *26*, 4521–4532.
(62) Kujawa, P.; Audibert-Hayet, A.; Selb, J.; Candau, F. *J. Polym. Sci., Part A: Polym. Chem.* **2003**, *41*, 3261–3274.
(63) Lacik, I.; Selb, J.; Candau, F. *Polymer* **1995**, *36*, 3197–3211.
(64) Regalado, E.; Selb, J.; Candau, F. *Macromolecules* **1999**, *32*, 8580–8588.
(65) Volpert, E.; Selb, J.; Candau, F. *Polymer* **1998**, *39*, 1025–1033.
(66) Volpert, E.; Selb, J.; Candau, F. *Macromolecules* **1996**, *29*, 1452–1463.
(67) Lara-Ceniceros, A. C.; Rivera-Vallejo, C.; Jimenez-Regalado, E. J. *Polym. Bull.* **2007**, *58*, 425–433.
(68) Rico-Valverde, J. C.; Jimenez-Regalado, E. J. *Polym. Bull.* **2009**, *62*, 57–67.
(69) Mather, B. D.; Elkins, C. L.; Beyer, F. L.; Long, T. E. *Macromol. Rapid Commun.* **2007**, *28*, 1601–1606.
(70) Several earlier models[3,73] were also considered for comparison with the data; all failed to capture an essential feature of the rheological master curves, namely the presence of relaxations at times much longer than that corresponding to the G'/G'' crossover. This crossover time scale is widely taken to represent τ_{max} due to the rapid transition to terminal behavior with decreasing frequency. In these UPy-based materials, however, a G'/G'' crossover is always seen, yet the transition to terminal behavior is often very broad or inaccessible even at high temperatures/low frequencies, particularly at high UPy concentration (see e.g. Figure 13).
(71) Variable temperature solid-state ^{1}H NMR experiments were performed on related materials (mono-end-functional PnBA) in which the UPy concentration in the melt is much lower and the equilibrium therefore shifted more toward unbound UPy. Even at temperatures as high as 120 °C no evidence of unbound UPy was seen, indicating an extremely high dimerization constant K_{dim} in the PnBA melt.
(72) Rubinstein, M.; Colby, R. *Polymer Physics*; Oxford University Press: New York, 2003.
(73) Baxandall, L. G. *Macromolecules* **1989**, *22*, 1982–1988.